Physics Letters A 375 (2011) 934–938

Contents lists available at ScienceDirect

Physics Letters A

www.elsevier.com/locate/pla

# Oxygen vacancy in $LiTiPO_5$ and $LiTi_2(PO_4)_3$: A first-principles study

Li-Juan Chen [a], Yu-Jun Zhao [a,*], Jia-Yan Luo [b], Yong-Yao Xia [b]

[a] Department of Physics, South China University of Technology, Guangzhou 510640, China
[b] Department of Chemistry and Shanghai Key Laboratory of Molecular Catalysis and Innovative Materials, Fudan University, Shanghai 2004339, China

ARTICLE INFO

*Article history:*
Received 8 March 2010
Received in revised form 21 December 2010
Accepted 26 December 2010
Available online 28 December 2010
Communicated by R. Wu

*Keywords:*
$LiTiPO_5$
$LiTi_2(PO_4)_3$
First-principles
Oxygen vacancy
Lithium-ion batteries

ABSTRACT

The structures of $LiTiPO_5$ and $LiTi_2(PO_4)_3$, as well as the possibility of oxygen vacancies formation in the systems are studied by first-principles calculations. It is found that oxygen vacancies can be formed in $LiTiPO_5$ and $LiTi_2(PO_4)_3$ under oxygen poor condition. The formation of oxygen vacancies introduce a defect band within their band gaps, which is expected to improve the electronic conductivity of $LiTiPO_5$ and $LiTi_2(PO_4)_3$ significantly. Meanwhile, a great concentration of oxygen vacancies may increase the discharge voltage of $LiTiPO_5$ and $LiTi_2(PO_4)_3$.



## 1. Introduction

Phosphate-based materials have generated considerable interest as potential cathode materials for secondary lithium batteries. This is primarily attributed to their competitive energy-density storage and better thermal properties than traditional cathode materials such as $LiCoO_2$, $LiMn_2O_4$ spinel, and $V_2O_5$ [1–6]. These materials take advantage of a relatively high lithium ion mobility and benefit from the inductive effect generated by their polyanionic groups, which increase the operating voltage in comparison with the simple oxides [1,2]. Recently, much attention has been focused on the phospho-olivine $LiMPO_4$ (M = Mn, Fe, Co and Ni) family of materials [3,6–12]. Good electrochemical performance has been reported for LISICON-type and NASICON-type materials such as $A_{1+x}M_2(PO_4)_3$ (A = Li, Na, M = Fe, V, Ti, Nb) [13–26]. Lithium transition metal phosphates suffer from low electrical conductivities and slow Li-ion diffusions that limit their rate capability. Past attempts to improve rate capability by increasing electrical conductivity have focused on coating particles with conductive carbons [27,28]. It is reported that the performance of many cathode materials are sensitive to the oxygen partial pressure during the sample preparation. For example, Wolfenstine et al. recently investigated the effect of heat-treatment under different oxygen partial pressures (pure oxygen, air, high-purity argon) on the discharge capacity of $LiCoPO_4$ and found that the samples heat-treated under low oxygen partial (high-purity argon) pressure exhibit a higher discharge capacity over the cycle range test compared to those prepared under air or pure oxygen [29]. The reason for the impact of oxygen partial pressure is not clear, although it was suggested due to formation of cobalt phosphides in $LiCoPO_4$, and titanium phosphides in $LiTi_2(PO_4)_3$ [29]. It is well known in metal oxides that oxygen vacancies are easy to form under oxygen poor condition and have critical roles in their electronic properties. Here we attempt to study the possibility of oxygen vacancy formation and its impact on the physical properties in $LiTiPO_5$ and $LiTi_2(PO_4)_3$, as the important Li battery cathode materials.

In this Letter, the crystal and electronic structure of $LiTiPO_5$ and $LiTi_2(PO_4)_3$, as well as the possibility of oxygen vacancy formation are investigated by the first-principles calculations. We find that in both $LiTiPO_5$ and $LiTi_2(PO_4)_3$, low oxygen partial pressure introduces oxygen vacancies in the crystals. These defects generate a defect band in both $LiTiPO_5$ and $LiTi_2(PO_4)_3$, which is expected to improve their conductivity significantly.

### 1.1. Computational details

The theoretical studies are conducted in the framework of density-functional theory combined with the generalized gradient approximation (GGA). All the calculations are done with the pseudopotential plane wave method [30] with the PW91 formulae [31], and the projector augmented wave (PAW) potentials, as implemented in the VASP code [32]. The charge density is obtained with an energy cut-off of 400.0 eV, and $\Gamma$-centered $4 \times 4 \times 4$ and $2 \times 2 \times 1$ $k$ meshes for $LiTiPO_5$ and $LiTi_2(PO_4)_3$, respectively, following the Monkhorst–Pack **k**-space integration method [33]. In the structure optimization, all the internal structural parame-

* Corresponding author. Tel.: +86 20 87110426; fax: +86 20 87112837.
*E-mail address:* zhaoyj@scut.edu.cn (Y.-J. Zhao).

0375-9601/$ – see front matter 
doi:10.1016/j.physleta.2010.12.063

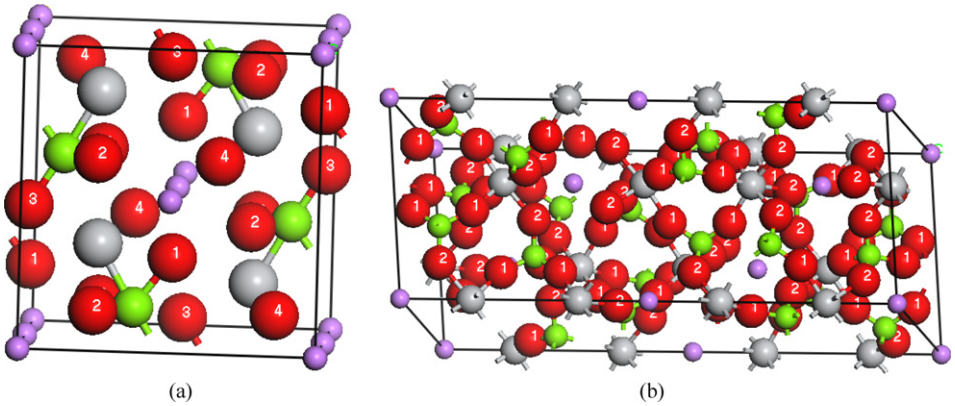


**Fig. 1.** Crystal structure of $LiTiPO_5$ (a) and $LiTi_2(PO_4)_3$ (b). The O, P, Ti, Li atoms are colored by red, green, gray, and orchid, respectively. (For interpretation of the references to color in this figure, the reader is referred to the web version of this Letter.)

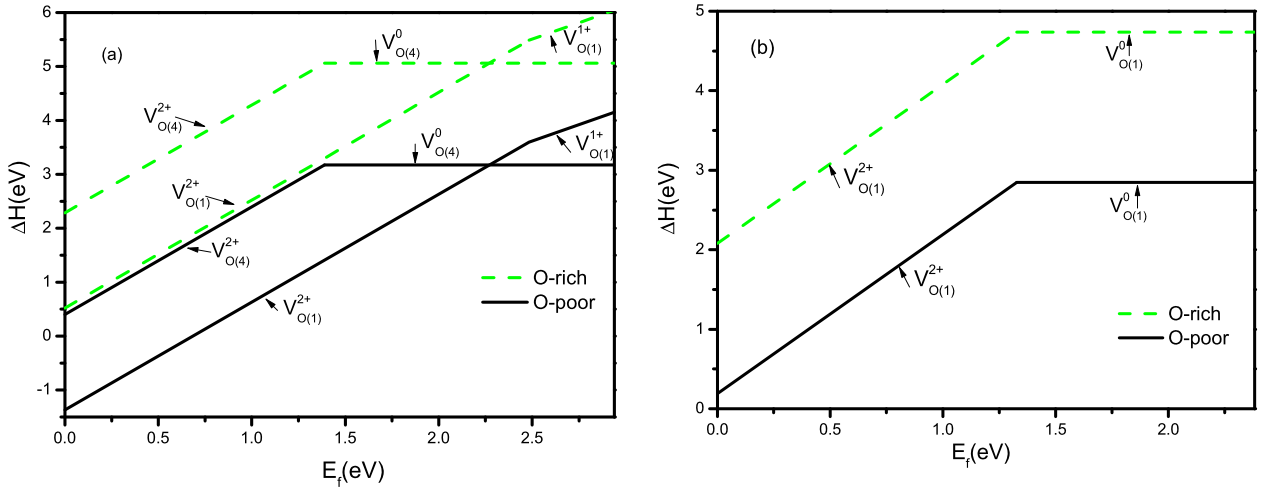


**Fig. 2.** The formation energy $\Delta H$ vs Fermi level for $LiTiPO_5$ (a) and $LiTi_2(PO_4)_3$ (b). $\Delta\mu_O$ is set to zero for O-rich condition while it is set to $-1.89$ eV for O-poor condition (corresponding to $T = 1000$ K, $p = 10^{-8}$ Pa).

ters are fully relaxed with the force convergence criterion of less than 0.02 eV/Å, while the lattice parameters are optimized with an energy criterion of less than 0.01 eV per molecular formula for $LiTiPO_5$ and $LiTi_2(PO_4)_3$. The density of states of the ideal and defected $LiTiPO_5$ and $LiTi_2(PO_4)_3$ are obtained with a $\Gamma$-centered $6 \times 6 \times 6$ and $4 \times 4 \times 2$ meshes, respectively.

## 2. Results and discussion

### 2.1. Crystal structure of $LiTiPO_5$ and $LiTi_2(PO_4)_3$

From X-ray diffraction studies [21] it is known that $LiTiPO_5$ has an oxotitanate cell, whose space group is Pnma (No. 62) and experimental lattice parameters are $a = 7.406$ Å, $b = 6.379$ Å, and $c = 7.238$ Å. The unit cell of $LiTiPO_5$ [shown in Fig. 1(a)] contains four formula units. All Li, Ti, and P atoms are equivalent respectively from the point view of symmetry, while there are four types of O atoms. For convenience, the four types of O ions are labeled as 1, 2, 3, and 4 in Fig. 1(a), respectively. $LiTi_2(PO_4)_3$ is isostructural with $NaZr_2(PO_4)_3$ [34] and adopts the well-known NASICON type structure consisting of a three-dimensional network made up of tetrahedra sharing all their corners with octahedra and vice versa to form the so-called "lantern" units, all oriented in the same direction along the **c**-axis. It is known that $LiTi_2(PO_4)_3$ is in the space group of $R\bar{3}C$ (No. 167) [23], whose experimental lattice parameters are $a_{hex} = 8.511$ Å, $c_{hex} = 20.843$ Å. The unit cell [shown in Fig. 1(b)] contains four formula units. All the Li, Ti, and P atoms are equivalent respectively in $LiTi_2(PO_4)_3$, while there are two types of O ions from the point view of symmetry. For convenience, the two types of O atoms are marked with 1 and 2 in Fig. 1(b). The lithium content will have a strong impact on the electrochemical behavior during Li insertion. The theoretical optimized lattice constants for $LiTiPO_5$ and $LiTi_2(PO_4)_3$ are listed in Table 1 along with the experimental values. Our theoretical results are in excellent agreement with the experiment data with errors of less than 1.3% for the lattice volume.

**Table 1**
Optimized and experimental lattice parameters for $LiTiPO_5$ and $LiTi_2(PO_4)_3$.

| | $a$ (Å) | $b$ (Å) | $c$ (Å) | Volume (Å$^3$) |
|---|---|---|---|---|
| $LiTiPO_5$ (Calc.) | 7.356 | 6.403 | 7.229 | 340.489 |
| $LiTiPO_5$ (Expt.) [24] | 7.406 | 6.379 | 7.238 | 341.944 |
| $LiTi_2(PO_4)_3$ (Calc.) | 8.534 | 8.534 | 20.457 | 1290.321 |
| $LiTi_2(PO_4)_3$ (Expt.) [26] | 8.511 | 8.511 | 20.843 | 1307.53 |

### 2.2. Possibility of oxygen vacancy formation in $LiTiPO_5$ and $LiTi_2(PO_4)_3$

In order to investigate the possibility of oxygen vacancy formation, we calculate the formation enthalpies ($\Delta H$) of O vacancy in $LiTiPO_5$ and $LiTi_2(PO_4)_3$ (shown in Fig. 2) according to the formula [35,36]

$$\Delta H_f^{(D,q)} = E(D,q) - E(0) + \sum_\alpha n_\alpha \left(\Delta\mu_\alpha + \mu_\alpha^{\text{Solid}}\right) + q(E_{\text{VBM}} + E_F) \quad (1)$$

where $E(D,q)$ and $E(0)$ are the total energies of the supercell with and without defect $D$. Here $(\Delta\mu_\alpha + \mu_\alpha^{\text{Solid}})$ is the absolute value of the chemical potential of atom $\alpha$. Also $n_\alpha$ is the number of atoms for each defect; $n_\alpha = -1$ if an atom is added, while $n_\alpha = 1$ if an atom is removed. $E_{\text{VBM}}$ represents the energy of the valance band maximum (VBM) in the defect-free system and $E_F$ is the Fermi energy relative to the $E_{\text{VBM}}$. The Fermi level could be self-consistently determined when all the defects are involved at a given growth condition. However, we only focus on the oxygen defects in this work, and thus the Fermi level is actually only a parameter between VBM and the conduction-band minimum (CBM) reflecting various samples prepared at different growth condition ($E_V \leqslant E_F \leqslant E_C$). The atomic structure was fully relaxed in our calculations.

The surrounding $O_2$ atmosphere is regarded as an ideal-gas-like reservoir. The temperature and pressure dependence for the chemical potential of oxygen, $(\Delta\mu_O + \mu_O^{\text{Solid}})$, may be expressed as following [37]

$$\mu_O(T,p) = \mu_O(T,p^0) + 1/2kT\ln\left(\frac{p}{p^0}\right). \tag{2}$$

The detailed numerical relation between $T$ and $\mu_O$ is discussed in Ref. [37]. Under the O rich condition, $\Delta\mu_O$ is set to zero and $\mu_O^{\text{Solid}} = 1/2E_{O_2}^{\text{total}} = \mu_O(0\text{ K}, p^0)$. The dependence of the formation enthalpy on the Fermi level is shown in Fig. 2 for oxygen vacancies in $LiTiPO_5$ and $LiTi_2(PO_4)_3$ under O-rich and O-poor conditions. Here O-poor condition is exemplified at $T = 1000$ K and $p = 10^{-8}$ Pa, a typical O-poor sample growth condition. From Fig. 2 we find that under the O-poor condition, O vacancies are able to form in both $LiTi_2(PO_4)_3$ and $LiTiPO_5$, especially in $LiTiPO_5$. The formation enthalpy of oxygen vacancies can be as low as 0.2 eV for $LiTi_2(PO_4)_3$, and even lower for $LiTiPO_5$ when the Fermi level is near VBM. When the Fermi level is close to CBM, oxygen vacancies are hard to form as the formation enthalpies are around 3.0 eV for both $LiTi_2(PO_4)_3$ and $LiTiPO_5$ even under O-poor condition. The O vacancies are mostly neutral charged when $E_F$ is close to the CBM, and they favor +2 charge state below mid-gap. In $LiTiPO_5$, the oxygen vacancies are relatively easy to form at O(1), O(2), or O(3) sites except that $E_F$ is near the CBM. The O-vacancy formation energies at O(2) and O(3) sites are not shown in Fig. 2 since they are similar to that of O(1). In $LiTi_2(PO_4)_3$, the formation energy of oxygen vacancy is always lower at the O(1) site when $E_F$ changes within the band gap. The stability of $V_O^{2+}$ is understandable since O-vacancies are expected to be a donor when $E_F$ is close to the VBM.

### 2.3. Influence of oxygen vacancy on the discharge voltage

From the electronic densities of states (DOS) in Fig. 3(a), we find that the ideal $LiTiPO_5$ has a calculated band gap of 2.94 eV and the experimental band gap is expected to be remarkably greater than the calculated one due to the well-known demerit of LDA/GGA on band gap evaluation. LDA + U or GGA + U may improve the description of the band gap and electronic structures for most transition metal (TM) oxides, especially the late TM oxides. However, for the systems of $LiTiPO_5$ and $LiTi_2(PO_4)_3$, LDA + U or GGA + U turns out not to improve the band gap remarkably since Ti is an early TM. For example, we have calculated the band-gap with GGA + U (U = 2.5 eV, as typically adopted in Ref. [38]) to be 2.91 eV for the ideal $LiTiPO_5$, no remarkable changes from the value obtained from GGA calculation. Thus GGA is still employed in this work. The obvious band gap indicates that the ideal $LiTiPO_5$ is expected to be an insulator, which will limit the electron mobility during the battery discharge. From Fig. 3(c), we find that the valence band around the Fermi level is mainly hybrided with titanium 3*d* states, phosphorus 3*p* states and oxygen 2*p* states, and the conduction bands are mainly made up by titanium 3*d* states

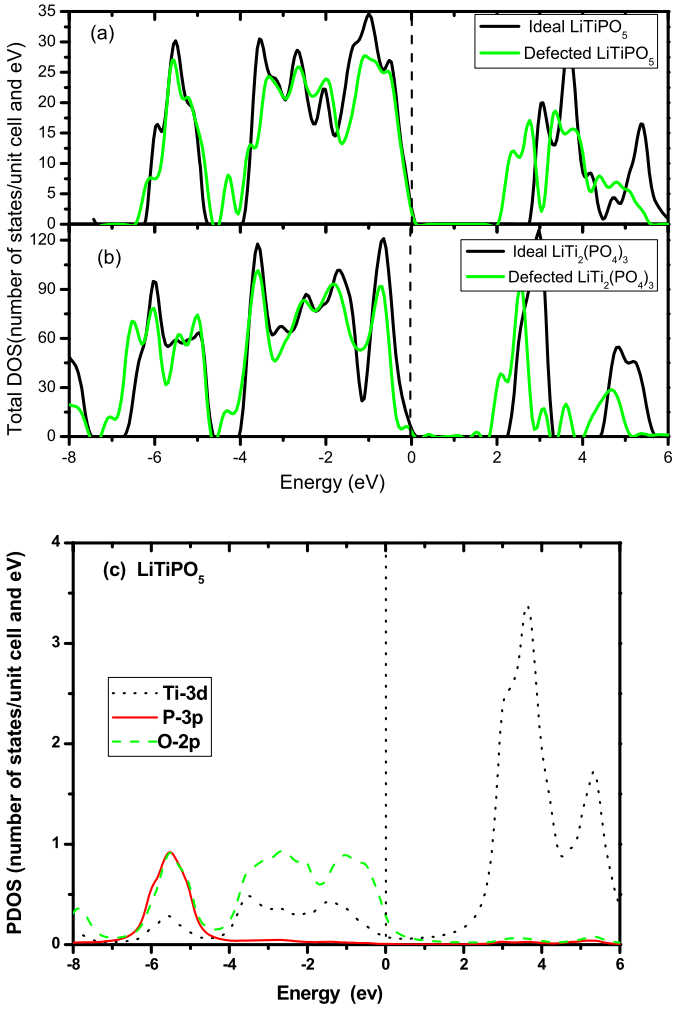


**Fig. 3.** (a) The total DOS of ideal and defected $LiTiPO_5$ and (b) the total DOS of ideal and defected $LiTi_2(PO_4)_3$, (c) the partial DOS of ideal $LiTiPO_5$.

in $LiTiPO_5$. By comparing the DOS of ideal $LiTiPO_5$ and defected $LiTiPO_5$, we observe that the defected $LiTiPO_5$ with O-vacancy has a band gap of 2.0 eV, which is significantly smaller than that of ideal $LiTiPO_5$. Fig. 3(b) shows the DOS of ideal $LiTi_2(PO_4)_3$ and defected $LiTi_2(PO_4)_3$. It indicates that $LiTi_2(PO_4)_3$ is an insulator with a calculated band gap of 2.38 eV in the ideal $LiTi_2(PO_4)_3$ and 1.94 eV in defected $LiTi_2(PO_4)_3$ with O-vacancy. In accordance with $LiTiPO_5$, O-vacancies significantly reduce the band gap of $LiTi_2(PO_4)_3$. Although the reduced band gap by O-vacancies in $LiTiPO_5$ and $LiTi_2(PO_4)_3$ will have no contribution for a better conductivity directly, it will increase the electron carriers by significantly reducing other possible donor levels. Our recent experiment also shows that the electronic conductivity of $LiTi_2(PO_4)_3$ is increased when the sample is heat-treated under $N_2$ atmospheres [39].

The discharge/charge voltage of the cathodic materials is controlled by the energy of active redox couple which varies from one material to another depending on two main factors [40]: (1) the electrostatic field at the cation position and (2) the covalent contribution to the cation–anion bonding. The discharge voltage, $V(x)$, actually depends on the value of $x$ in $Li_xTiPO_5$ or $Li_xTi_2(PO_4)_3$ since the chemical potential of Li is a function of $x$, similarly to the case of $Li_xMPO_4$ discussed in Ref. [40]. The detailed expression for the discharge voltage can be written as following [41]

$$V(x) = -\frac{1}{F}\left(\frac{\delta\Delta G(x)}{\delta x}\right)_{T,P}, \tag{3}$$

where $F$ is the Faraday constant and $\Delta G(x)$ is the change in Gibb's free energy for the intercalation reaction,

$$\delta x\mathrm{Li} + \mathrm{Li}_x\mathrm{TiPO}_5 \rightarrow \mathrm{Li}_{x+\delta x}\mathrm{TiPO}_5; \tag{4}$$

or

$$\delta x\mathrm{Li} + \mathrm{Li}_x\mathrm{Ti}_2(\mathrm{PO}_4)_3 \rightarrow \mathrm{Li}_{x+\delta x}\mathrm{Ti}_2(\mathrm{PO}_4)_3. \tag{5}$$

The detailed calculation of Gibb's free energy as a function of $x$ is complicated due to lack of practical ordering of Li ions at any value of $x$, which requires a comprehensive Monte Carlo simulation. Fortunately, the calculation of the average intercalation voltage through first-principle has been proposed in Ref. [42] Generally, Gibb's free energy contributions from the volume changes and entropy associated with the intercalation are negligibly. Otherwise, the stability of the cathode materials will be a critical issue. Therefore, the average discharge voltage in a fully Li discharge procedure for $\mathrm{LiTiPO}_5$ or $\mathrm{LiTi}_2(\mathrm{PO}_4)_3$ (cf. Eqs. (4)–(5)) can be deduced from the change of the internal energy $\Delta E$ at 0 K, i.e.:

$$\overline{V} \approx -\frac{\Delta E}{F}. \tag{6}$$

Here $\Delta E$ is given by the total energy difference between $\mathrm{Li}_2\mathrm{TiPO}_5$ and the sum of $\mathrm{LiTiPO}_5$ and metallic lithium for $\mathrm{LiTiPO}_5$, while it is given by the energy difference between $\mathrm{Li}_3\mathrm{Ti}_2(\mathrm{PO}_4)_3$ and the sum of $\mathrm{LiTi}_2(\mathrm{PO}_4)_3$ and metallic lithium for $\mathrm{LiTi}_2(\mathrm{PO}_4)_3$. Experimentally, it is hard to realize the "lithium-stuffed" composition $\mathrm{Li}_2\mathrm{TiPO}_5$ [21]. Therefore, we estimate its discharge voltage by inserting Li atoms into $\mathrm{LiTiPO}_5$ lattice.

The study of both factors can be properly accomplished on oxides formed by $\mathrm{MO}_6$ octahedra (M = transition metal cation) linked by tetrahedral polyanions ($\mathrm{XO}_4^{n-} = \mathrm{PO}_4^{3-}$, $\mathrm{AsO}_4^{3-}$, $\mathrm{SO}_4^{2-}$, etc.) [41]. The calculated average voltage for $\mathrm{Li/LiTiPO}_5$ with O-vacancy free is 0.68 V, and it is increased by 15% to 0.78 V for the system with O-vacancy. In general, the GGA calculated voltage of delithium is lower than the experimental measurement. In $\mathrm{Li/LiTiPO}_5$ case, the experimental observed voltage of delithium is to be 1.51 V [21]. In our calculations, it is found that the lengths of two different Ti–O bonds next to the O-vacancy decreased with 11.1% and 3.7% in the system, respectively, compared to the corresponding bonds without O-vacancy in $\mathrm{LiTiPO}_5$. Furthermore, the calculated lengths of the Li–Li bonds in $\mathrm{LiTiPO}_5$ with O-vacancy are decreased by 0.3 Å and 0.23 Å, i.e., 9.4% and 7.2%, respectively. We find that the total charge around Ti decreases in $\mathrm{LiTiPO}_5$ when O-vacancies are introduced. Thus, the oxidation state of Ti is expected to be increased.

The calculated average voltage of the system $\mathrm{Li/LiTi}_2(\mathrm{PO}_4)_3$ is 1.26 V in the system without O-vacancy and is increased by 11.1% to 1.42 V for the system with O-vacancy. Clearly, GGA tends to underrate the average delithium voltage for $\mathrm{Li}_3\mathrm{Ti}_2(\mathrm{PO}_4)_3$ with respect to the experimental value of 2.48 V reported in Refs. [21,43]. Meanwhile, the imperfect crystal phase of the experimental samples may also contribute to the discrepancy of the voltage. In comparison with the ideal $\mathrm{LiTi}_2(\mathrm{PO}_4)_3$, the bond length of Ti–O closest to the O-vacancy decreases by 7.6%. The bond length of P–O closest to the O-vacancy also decreases by 3.7%. However, the charge of Ti ions near the O-vacancy increases, while that of other Ti ions decreases in $\mathrm{LiTi}_2(\mathrm{PO}_4)_3$ with O-vacancy after delithium, in comparison with the corresponding Ti total charge in ideal $\mathrm{LiTi}_2(\mathrm{PO}_4)_3$. This may result in the decrease of the total charge around Ti and leads to the increase of the Ti redox voltage.

## 3. Conclusion

In conclusion, by means of first-principles theory, we have calculated the crystal constants and volumes of ideal $\mathrm{LiTiPO}_5$ and $\mathrm{LiTi}_2(\mathrm{PO}_4)_3$ systems, which are in good agreement with available experiment values. Our calculated results indicate that oxygen vacancies may be formed under extreme O-poor condition in $\mathrm{LiTi}_2(\mathrm{PO}_4)_3$ and particularly in $\mathrm{LiTiPO}_5$. Their electronic conductivity is expected to increase in comparison with the ideal $\mathrm{LiTiPO}_5$ and $\mathrm{LiTi}_2(\mathrm{PO}_4)_3$ respectively, since the band gaps of the systems are significantly reduced by the defect band introduced by oxygen vacancies. The discharge voltages of $\mathrm{LiTiPO}_5$ and $\mathrm{LiTi}_2(\mathrm{PO}_4)_3$ may be increased due to possible large concentration of oxygen vacancies. It is expected that the impact of the defects to the electronic conductivity will stimulate further experimental research on the promising spinel and olivine structural cathode materials, such as $\mathrm{LiTiPO}_5$ and $\mathrm{LiTi}_2(\mathrm{PO}_4)_3$.

## Acknowledgements

This work was financially supported by the National Natural Science Foundation of China (NSFC) under Grant No. 1074025 and the Fundamental Research Funds for the Central Universities, SCUT, under project 2009ZZ0068. We thank the computer time at the High Performance Computer Center of Shenzhen Institute of Advanced Technology (SIAT), Chinese Academy of Science.

## References

[1] A.K. Padhi, K.S. Nanjundaswamy, J.B. Goodenough, J. Electrochem. Soc. 44 (1997) 1188.
[2] A.K. Padhi, K.S. Nanjundaswamy, C. Masquelier, S. Okada, J.B. Goodenough, J. Electrochem. Soc. 144 (1997) 1609.
[3] A. Yamada, S.C. Chung, K. Hinokuma, J. Electrochem. Soc. 148 (2001) A224.
[4] M. Takahashi, S.-I. Tobishima, K. Takei, Y. Sakurai, Solid State Ionics 148 (2002) 283.
[5] E. Zhecheva, M. Mladenov, P. Zlatilova, et al., J. Phys. Chem. Solids 71 (2010) 848.
[6] J.Y. Li, W.L. Yao, S. Martin, D. Vaknin, Solid State Ionics 179 (2008) 2016.
[7] M. Piana, M. Arrabito, S. Bodoardo, A. D'Epifanio, D. Satolli, F. Croce, B. Scrosati, Ionics 8 (2002) 17.
[8] G. Li, H. Azuma, M. Tohda, Electrochem. Solid State Lett. 5 (2002) A135.
[9] S. Okada, S.I. Sawa, Y. Uebou, M. Egashira, J.I. Yamaki, M. Tabuchi, H. Kobayashi, K. Fukumi, H. Kageyama, Electrochemistry 71 (2003) 1136.
[10] T.G. Xu, L.B. Wang, S. Li, C.A. Ma, Acta Chimica Sinica 67 (2009) 2275.
[11] Z. Su, S.H. Ye, Y.L. Wang, Chinese J. Inorganic Chem. 26 (2010) 693.
[12] G.Y. Chen, T.J. Richardson, J. Power Sources 195 (2010) 1221.
[13] J. Gaubicher, C. Wurm, G. Goward, C. Masquelier, L. Nazar, Chem. Mater. 12 (2000) 3240.
[14] S. Patoux, C. Wurm, M. Morcrette, G. Rousse, C. Masquelier, J. Power Sources 119/121 (2003) 279.
[15] H. Ohkawa, K. Yoshida, M. Saito, K. Uematsu, K. Toda, M. Sato, Chem. Lett. 10 (1999) 1017.
[16] M. Sato, H. Ohkawa, K. Yoshida, M. Saito, K. Uematsu, K. Toda, Solid State Ionics 135 (2000) 137.
[17] M.Y. Saïdi, J. Barker, H. Huang, J.L. Swoyer, G. Adamson, Electrochem. Solid State Lett. 5 (2002) A149.
[18] H. Huang, S.-C. Yin, T. Kerr, N. Taylor, L.F. Nazar, Adv. Mater. 14 (2002) 1525.
[19] M.Y. Saïdi, J. Barker, H. Huang, J.L. Swoyer, G. Adamson, J. Power Sources 119/121 (2003) 266.
[20] J.C. Zheng, X.H. Li, Z.X. Wang, et al., Ionics 16 (2009) 753.
[21] S. Patoux, C. Masquelier, Chem. Mater. 14 (2002) 5057.
[22] G.X. Wang, D.H. Bradhurst, S.X. Dou, H.K. Liu, J. Power Sources 124 (2003) 231.
[23] A. Aatiq, M. Ménétrier, L. Croguennec, E. Suard, C. Delmas, J. Mater. Chem. 12 (2002) 2972.
[24] X.M. Wu, R.X. Li, S. Chen, Z.Q. He, Rare Metals 28 (2009) 122.
[25] C.M. Burba, R. Frech, Solid State Ionics 177 (2006) 1489.
[26] J.K. Sun, F.Q. Huang, Y.M. Wang, et al., J. Alloys, Compounds 469 (2009) 327.
[27] N. Ravet, Y. Chouninard, J.F. Magnan, S. Besner, M. Gauthier, M. Armand, J. Power Sources 97/98 (2001) 503.
[28] H. Huang, S.-C. Yin, L.F. Nazar, Electrochem. Solid State Lett. 4 (2001) A170.
[29] J. Wolfenstine, U. Lee, B. Poese, J.L. Allen, J. Power Sources 144 (2005) 226.
[30] J. Ihm, A. Zunger, M.L. Cohen, J. Phys. C 12 (1979) 4409.
[31] J.P. Perdew, Y. Wang, Phys. Rev. B 45 (1992) 13244.
[32] G. Kresse, J. Hafner, Phys. Rev. B 47 (1993) 558;
G. Kresse, J. Furthmüller, Phys. Rev. B 54 (1996) 11169.
[33] H.J. Monkhorst, J.D. Pack, Phys. Rev. B 13 (1976) 5188.
[34] L.O. Hagman, P. Kierkegaard, Acta Chem. Scand. 22 (1968) 1822.

[35] S.B. Zhang, S.-H. Wei, A. Zunger, H. Katayama-Yoshida, Phys. Rev. B 57 (1998) 9642.
[36] S.B. Zhang, S.-H. Wei, A. Zunger, Phys. Rev. Lett. 78 (1997) 4059.
[37] K. Reuter, M. Scheffler, Phys. Rev. B 65 (2001) 035406.
[38] I.V. Solovyev, P.H. Dederichs, a.V.I. Anisimov, Phys. Rev. B 50 (1994) 16861.
[39] Jia-Yan Luo, Li-Juan Chen, Yu-Jun Zhao, Ping He, Yong-Yao Xia, J. Power Sources 194 (2009) 1075.
[40] O. Garcia-Moreno, M. Alvarez-Vega, F. Garcia-Alvarado, et al., Chem. Mater. 13 (5) (2001) 1570.
[41] J.M. Osorio-Guillén, B. Holm, et al., Solid State Ionics 167 (2004) 221.
[42] G. Ceder, Y.M. Chiang, D.R. Sadoway, et al., Nature (London) 392 (1998) 694.
[43] Jia-Yan Luo, Yong-Yao Xia, Adv. Func. Mater. 17 (18) (2007) 3877.